Understanding Fire Growth for Performance Based Design of Bamboo Structures

Angela Solarte[a,*], Aaron Bolanos[a], Janal Numapo[a], Tam Do[a], Juan P. Hidalgo[a], Jose L. Torero[b]

[a]University of Queensland, Australia, a.solartecastaneda@uq.edu.au

[b]University of College London, London, j.torero@ucl.ac.uk

Abstract:

This paper analyses the different parameters governing fire growth and presents the quantification of these parameters for laminated bamboo samples produced from the species *Phyllostachys pubescens* "Moso". Parameters such as critical heat flux, temperature for ignition, thermal inertia, mass loss rate and heat release rates are studied herein. Last, the ignition parameters of laminated bamboo are contrasted against the available information on bamboo and commonly used timber products.

Keywords: laminated bamboo; pyrolysis; ignition: fire growth; heat transfer; burning rates; heat release rates;

1. Introduction

Material developers have created novel construction products such as laminated bamboo, bamboo scrimber, and bamboo oriented strand boards [1]. These products are being used as construction materials in residential, office, airports, and hotel buildings, among other [2, 3]. Studies have shown that bamboo is not only a more renewable and sustainable material than timber [4, 5], but it has also proven to have good mechanical properties relative to wood [6-8]. As a result, bamboo is becoming a very appealing material for structural applications in construction [9], as it provides an opportunity for modern multi-story buildings to be designed with bamboo as a key component. Bamboo is heavily used in developing countries, mainly Southeast Asia and South America, and it has the potential to grow in the market as manufacturers further develop the technology to construct robust laminated bamboo products. The main species of bamboo used as "timber" are *Phyllostachys pubescens* "Moso" and *Guadua angustifolia kunth,* the former comes mainly from China and the latter grows in Central and South America. China is still the principal producer and manufacturer of bamboo products globally and supplies construction materials like flooring and engineering bamboo to Australia, India and Western Europe [10].

The development of new materials is generally focused on its functional properties and therefore it usually introduces a gap of knowledge in relation to their fire behaviour. Therefore, these novel materials when included in designs and construction without the proper understanding, can result in unquantified risks.

Fig. 1 illustrates how the introduction of a novel material with unknown fire behaviour may raise many uncertainties. For example, Available Safe Egress Times (ASET) may shorten if ignition and growth phase is faster. Then the values of the Required Safe Egress Time (RSET) may no longer be enough to egress safely. In addition, the size of the fire could be bigger than expected and the fire load received by the structural members could generate failure of the structure. As the energy delivered to the structure could be of a higher magnitude and last for a longer period, affecting neighbouring buildings and fire fighters attending the scene.

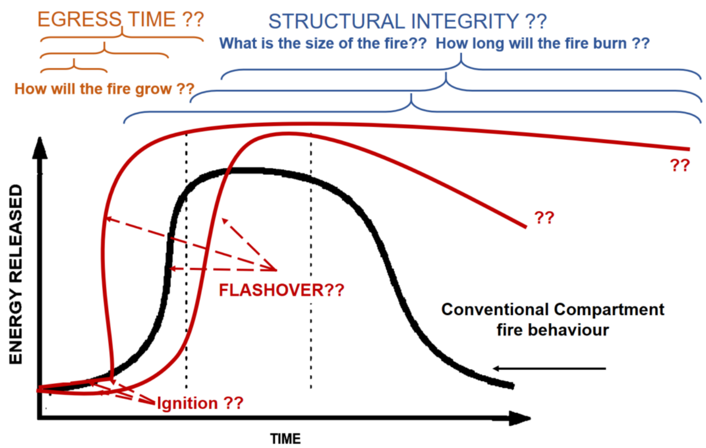

Fig. 1 Uncertainties of the fire dynamics when unknown material's fire behaviour

In order to achieve a fire safe design, it is important to understand the changes in the fire dynamics of a compartment that will come as a consequence of including laminated bamboo as a lining, finishing or structural element. It is crucial to know how bamboo can influence ignition times, and the effect that bamboo will have in the growth of the fire, as well as its contribution to accelerate flashover. Therefore, it is crucial to develop knowledge on the fire performance of engineering bamboo products.

1.1. General Approach

This paper presents a characterisation of the fire performance of laminated bamboo. The primary objective of this paper is to quantify the flammability parameters that drive the growth phase of a fire, as a starting point to build an understanding of the failure modes when including laminated bamboo in a compartment as a finishing or structural element. By doing so, the design of fire-safe bamboo structures can be articulated in performance-based terms. Processes such as ignition, flame spread and Heat Release Rates dominate the growth of a fire, while fuel loads, burning rates and ventilation its ultimate duration [17]. While it is difficult to quantitatively predict fire growth in terms of fundamental parameters, it is clear that these processes are controlled by a series of well-defined parameters [17]. Therefore, parameters such as critical heat flux for ignition, ignition temperature, thermal inertia, burning rates, and heat release rate will be determined using an experimental approach based on Cone Calorimeter (ISO 5660) [11].

2. Material and Methods

2.1. Materials

Three different samples types of laminated bamboo *Phyllostachys pubescens* (Moso), were tested in a horizontal configuration as shown in **Error! Reference source not found.**.**Error! Reference source not found.**

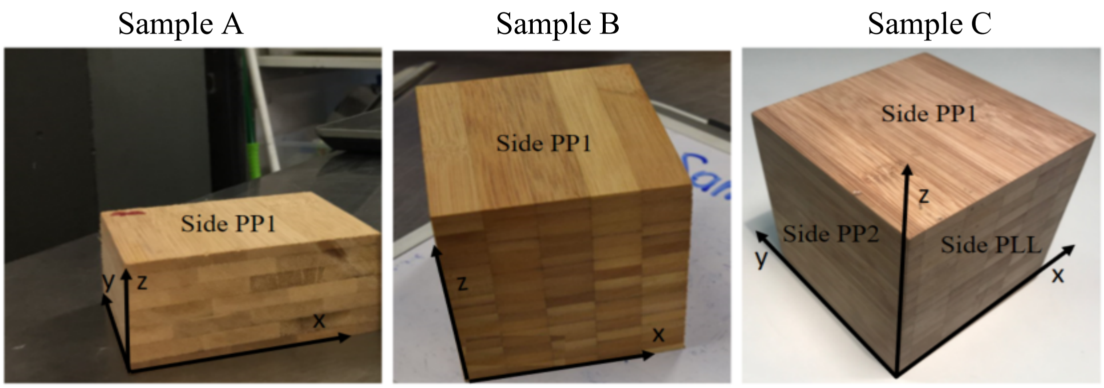

Fig. 2. Laminated Bamboo sample tested a) Sample A, b) Sample B, c) Sample C

Sample A and B were tested perpendicular to the grain (PP1), with the bamboo strips placed flatwise. Sample C was tested perpendicular (PP1, PP2) and parallel to the grain (PLL). As seen in Fig. 2, side PP1 and PP2 refer to the surface that is exposed perpendicularly to the fibre with bamboo strips positioned flatwise (surface xy) and edgewise (surface yz) , respectively, while side PLL is the nomenclature assigned to the surface that has been exposed in a parallel way (surface xz). Sample A was 40 mm thick and Sample B and C 100 mm thick. **Error! Reference source not found.** describes each of the samples.

Table 1 Description of samples

Sample	Adhesive	Density [kg/m^3]	Moisture Content [%]	Surface area [m^2]
A	Urea Formaldahyde	575 ± 15	7.17 ± 0.06	$8.1x10^{-3}$±$5.4x10^{-4}$
B	Phenol Resorcinol formaldahyde	693 ± 16	6.08 ± 0.40	$9.0x10^{-3}$± 1.5 $x10^{-3}$
C	Phenol Formaldahyde	734 ± 20	8.12 ± 0.02	$1.0x10^{-2}$ ± 7.8 $x10^{-5}$

2.2. Experimental Set-Up

Tests to characterise the fire behaviour of laminated bamboo were conducted in the cone calorimeter with a horizontal configuration. Samples were covered with aluminium foil on the sides and the back to achieve uniform heating only at the surface. To guarantee pilot ignition, a 10 kV spark placed 13 mm above the centre of the sample's surface was activated at the start of the test until ignition was achieved.

The samples were tested for different heat fluxes starting from 10 kW/m^2 and up to 80 kW/m^2. Each heat flux value was calibrated prior to the tests by measuring the heat flux with a water cooled heat flux gauge of the Schmidt-Boelter type. The heat flux gauge was placed inside the chamber 25 mm away from the radiant heater.

During the tests, the time to ignition was observed and recorded. After ignition started, the spark was removed from the sample, allowing the sample to burn. The tests were stopped after 30 minutes if no ignition was achieved, according to BS ISO 5560-1:2015 [11]. The mass of the sample was measured, and flameout times were recorded. Products from the combustion process, including oxygen, carbon monoxide and carbon dioxide were gathered and measured inside a 114 mm diameter exhaust duct system with a nominal flow rate of 24 l/s before being sucked by a 400 mm x 400 mm extraction hood.

To calculate the heat release rate of the test, the combustion gases were collected and directed into a gas-sampling ring. Prior to this, gases are filtered before reaching the gas analysers to remove all particles and as much water as possible [12]. During the tests, the gas-sampling ring used moisture removal traps, such as Balstron filter, Hepa Vent, a cold trap, and two sampling drying columns that use Drierite as the drying agent, to filter the combustion gases before reaching the gas analyser. The Servomex Gas Analyser was used to process the products such as oxygen, carbon dioxide and carbon monoxide. A data logger was used to record all the information. The gas analysis readings were correct at the end of each test, the sample was removed before stopping the tests readings, and the concentration of oxygen was observed to return to the original calibrated value of 20.95%. If the readings were different, the data for heat release rate was deemed invalid, and the test was repeated.

2.3. Ignition Model

A brief summary of ignition theory will be presented to extract the parameters controlling ignition. A detail description of ignition theory can be found in [13-15]. When energy is applied to the surface of a solid, heat is diffused through the material, eventually heating the whole thickness. The region that has been heated by the thermal wave is referred to as the characteristic length (ε_T), which is as a function of the Fourier number (time and thermal diffusivity). In the case where the characteristic length is much smaller than the sample length, the sample acts as a semi-infinite solid ($L > \varepsilon_T$). This means that the thickness of the material is considered infinite, as the back never sees the thermal wave. Since many materials will not present an infinite thickness behaviour, a characteristic time, t_c, during which the material will behave as a semi-infinite solid needs to be considered [16]. By assuming that solids will show little evidence of decomposition and onset of chemical reactions prior to reaching its pyrolysis temperature, the material is assumed inert [13, 17]. Furthermore, if the solid is assumed not to react until the surface reaches the ignition time, the energy required for pyrolysis can be ignored. Equations (1), (2), (3) show the partial differential equation of the energy balance in the inert solid and limited by the boundary conditions:

$$k \frac{\partial^2 T}{\partial x^2} = \rho C_p \frac{\partial T}{\partial t} \tag{1}$$

$$for\ x = 0; t = 0 \qquad \dot{q}''_{net} = -k \frac{\partial T}{\partial x} \tag{2}$$

$$for\ x = L \rightarrow \infty; \qquad \dot{q}''_{net} = -k \frac{\partial T}{\partial x} = 0; \qquad T = T_\infty \tag{3}$$

where k is the thermal conductivity of the solid [W/mK], ρ the density of the solid [kg/m³], C_p the specific heat of the solid [J/kgK], and $\partial T/\partial x$ the themal gradiant at the surface. The Laplace transformation of the previous equations permits to find T_{ig} [18]. Equation (4) provides an expression that solves for the surface temperature at all levels of the external heat flux. $\bar{T}$ is defined as a characteristic temperature, t_c is a characteristic time defined as a function of the thermal inertia $k\rho C_P$ and heat transfer, and erfc is the complementary Gaussian error function [15]:

$$T_{ig} = T_\infty + \bar{T}\left[1 - e^{\left(\frac{t_{ig}}{t_c}\right)} erfc\left(\left(\frac{t_{ig}}{t_c}\right)^{\frac{1}{2}}\right)\right] \text{ where } \bar{T} = \frac{\alpha \dot{q}_e''}{h_T}\text{ ;} \qquad t_c = \frac{k\rho C_P}{h_T^2} \quad (4),(5)$$

where t_c is the characteristic time or the time in which the thermal wave moves in the depth of the thickness of the material. Solving equation (4) using a first-order Taylor series expansion, provides various solutions. When the characteristic time is much larger than ignition times [$t_{ig}/t_c \rightarrow 0$] corresponds to a scenario for high external heat fluxes that are proportional to the inverse of the ignition time as seen in equation (6).

$$\frac{1}{\sqrt{t_{ig}}} = \frac{2}{\sqrt{\pi}}\frac{\alpha}{\sqrt{k\rho C_p}}\frac{1}{[T_{ig} - T_\infty]}\dot{q}_e''; \qquad \frac{1}{\sqrt{t_{ig}}} = \frac{\sqrt{\pi}\sqrt{k\rho C_P}}{h_T}\left[1 - \frac{h_T(T_{ig} - T_\infty)}{\alpha \dot{q}_e''}\right] \quad (6),(7)$$

Second when $t_{ig}/t_c \rightarrow \infty$, the characteristic time is much smaller than ignition times. This solution depends on the global heat transfer coefficient and is applied for lower heat fluxes as shown in equation ,(7). If the delay ignition time is considered infinite ($t_{ig} \rightarrow \infty$), equation ,(7) allows determining a critical heat for ignition. The critical heat flux for ignition represents the minimum external heat flux by which T_{ig} will be achieved at thermal equilibrium. From equation (8), the critical heat flux for ignition can be easily determined experimentally, which facilitates calculation of the temperature for ignition, a more difficult parameter to obtain by means of laboratory testing.

$$\dot{q}_{cr}'' \approx \frac{h_T(T_{ig} - T_\infty)}{\alpha} \quad \rightarrow \quad T_{ig} \approx T_\infty + \frac{\alpha \dot{q}_{cr}''}{h_T} \quad (8)$$

Form equations (6) and ,(7) the thermal inertia or $k\rho C_P$, refers to the ability of a material to resist the change in its own temperature. To determine the thermal inertia, a linear regression analysis for a given set of heat fluxes and ignition times is completed following equation (6). This analysis yields a value referred to as the 'effective' thermal inertia ($k\rho C_P$), which is a quantitative property that can be used to compare different materials within the scope of assumptions and simplifications explained previously.

2.4. Fire point theory: critical mass loss rate for ignition

The existence of a minimum mass loss rate to characterise the onset of ignition was first suggested by Bamford et al. [19] in 1946 . Kanury stated that in the threshold of ignition, the pyrolysis rate was expected to be increased so much that the resulting mixture of gases reaches concentrations above the lower flammability limits [20]. However, it was Rasbash that described a detailed concept that successfully allowed the use of a critical mass loss flux at the fire-point as the threshold value to describe the beginning of sustained flaming combustion [21, 22], were the burning rate heat balance at the surface of a solid fuel is given by equation (9) [23].

$$\dot{m}'' = \frac{\dot{Q}_E'' + \dot{Q}_{Flame}'' - \dot{Q}_{Loss}''}{L_V} \tag{9}$$

Here $\dot{m}''$ is the mass loss rate of the production of volatiles [g/m^{2}s], $\dot{Q}_E''$ the external heat flux [kW/m^2], $\dot{Q}_{Flame}''$ the heat flux supplied by the flame [kW/m^2], $\dot{Q}_{Loss}''$ the heat losses through the surface [kW/m^2] and L_V is the heat required to produce volatiles [kJ/g]. If $\dot{Q}_E'' + \dot{Q}_{Flame}'' > \dot{Q}_{Loss}''$, then burning will continue until $\dot{m}''$ reaches the threshold of the critical mass loss rate, $\dot{m}_{cr}''$ [g/m^{2}s]. This threshold can cause the flame to extinguish because the heat losses are greater than the heat to sustain the production of volatiles [23]. When the external heat flux is removed, ($\dot{Q}_E'' = 0$), the flames will continue to burn only under the conditions in equation (10).

$$\dot{m}_{cr}'' < \frac{\dot{Q}_{Flame}'' - \dot{Q}_{Loss}''}{L_V} \tag{10}$$

Rasbash et al. proposed that by experimentally measuring the mass loss rate for piloted ignition, determining $\dot{m}_{cr}''$ was possible. The set-up of his testing included a radiant heating panel, a load cell to monitor the weight and a pilot ignitor [24]. They stated that the mass loss measured would eventually reach a critical mass flow of fuel volatiles at the firepoint, point at which combustion produces enough heat to sustain the generation of volatiles from the solid to sustain the flame [24].

To determine the critical mass loss rate ($\dot{m}_{cr}''$) of laminated bamboo, the mass loss was measured in a 1-second interval for all samples during pilot ignition using the Cone Calorimeter. With the use of a load cell the weight of the sample was recorded while being exposed to 10-80kW/m^2 heat fluxes. The mass loss rate per unit area was obtained by differentiation of the mass over the time step and divided by the exposed surface area of the sample. The mass loss rate per unit area (g/m^{2}s) calculated over each second was graphed vs time (s). A typical mass loss rate profile is one were the mass loss rate increases gradually before achieving a steep increment around the time in which the sample ignited [24]. The critical mass loss rate for ignition ($\dot{m}_{cr}''$) in the laminated bamboo samples was obtained at the inflection point where ignition takes place.

2.5. Heat Release Rate: Oxygen consumption

To obtain the heat release rate of laminated bamboo, experiments were conducted in the Cone Calorimeter as explained in section 2.2. The heat released rate determines the size of the fire and correct understanding of its magnitude is critical to be able to create fire safe designs [25]. Many authors have suggested the determination of the heat release rate based on oxygen consumption [26, 27]. Initial results suggested that by calculating the unit mass of oxygen consumed in combustion, it was possible to determine the amount of energy released [28]. Parker [29], produced a series of formulations based on equation (11), where oxygen concentration inside an exhaust duct was calculated by differentiation of the volume flow of air into the system and the volume flow of combustion gases into the exhaust duct.

$$\dot{Q} = \left(X_{o_2}^{o}\dot{V}_o - X_{o_2}^{s}\dot{V}_s\right)\rho_{o_2}E \tag{11}$$

where $X^o_{O_2}$ is the oxygen concentration of air, $X^s_{O_2}$ the oxygen concentration in the duct, $\dot{V}_o$ the volume flow of air into the system at ambient [m^3/s], $\dot{V}_s$ the volume flow of gas in the exhaust duct at ambient [m^3/s], ρ_{o_2} the density of oxygen at ambient [kg/m^3], and E the heat produced per unit mass of oxygen consumed. Based on findings by Hugget [30], if the heat of combustion of a burning fuel, Δh_c, and its stoichiometric oxygen to mass of oxygen, r, are known; the heat produced per unit mass of oxygen consumed, E, is given by $\Delta H/r$. Otherwise, E is assumed as 13.1 MJ/kg. According to Babrauskas [31], the heat release can be found from equation (12) where the heat release rate is given by calculating the mass of oxygen.

$$\dot{Q} = \left(\frac{\Delta h_c}{r_o}\right) x\left(\dot{m_{O_{2,\infty}}} - \dot{m_{O_2}}\right) \quad (12)$$

Here $\dot{Q}$ is the heat release rate [kW], $\Delta \mathrm{h}_c$ is the net heat of combustion [kJ/kg], r_o the stoichiometric oxygen/fuel mass ratio, $\dot{m_{O_{2,\infty}}}$ the mass of oxygen at ambient conditions calibrated before the test (20.95%), $\dot{m_{O_2}}$ the mass of oxygen during the test. Based on the fact that most fuels generate 13.1 MJ/kg of energy on every kilogram of oxygen that is consumed [30, 32], therefore, $\Delta h_c/r_o$ is equal to 13.1 MJ/kg. Hence, the previous equation simplifies to equation (13), where $\dot{m_{O_{2,\infty}}}$ and m_{O_2} are values measured in the cone calorimeter.

$$\dot{Q} = 13.1x10^3 x\left(\dot{m_{O_{2,\infty}}} - \dot{m_{O_2}}\right) \quad (13)$$

3. Results

3.1. Validation of assumptions

Assumptions presented in section 2.2 addressed simplifications 1-3 in detail. However, to validate assumption 4, measuring the temperature evolution inside the solid was conducted for each tested sample type.

1. The solid is considered inert until ignition,
2. Ignition will occur at the onset of pyrolysis
3. Pyrolysis will be accomplished when the surface reaches the ignition temperature.
4. The sample is a semi-infinite solid,

The time, in which the material behaved as a semi-infinite solid, was determined by tracking the thermal wave using type K thermocouples for low, medium and high magnitudes of heat flux. Samples that have the minimum and maximum thickness (0.04 and 0.1 m), namely A and C respectively, were tested using the relevant orientation as presented in Table 2. Analysis of the data was done taken into consideration these characteristic times for each sample type.

Table 2. Characteristic times for Sample A and Sample C

Heat Flux	Samples	Time [s]	Heat Flux	Side	Time [s]
10kW/m^2	S.A_PP1	1,400	15kW/m^2	S.C_PP1	8,500
				S.C_PLL	4,500
45kW/m^2	S.A_PP1	550	80kW/m^2	S.C_PP1	3,600

				S.C_PLL	2,750

It was determined that sample A was able to be analysed as a semi-infinite solid, only during ignition process, as the thermal wave arrived to the back before flameout was completed. Due to this fact, no results for the heat release rate will be presented for sample A.

3.2. Ignition

3.2.1. Ignition

The critical heat flux for ignition is the maximum value of heat flux for which no ignition is recorded [11, 33]. For Sample A, B and C tested perpendicular to the grain PP1 and PP2 the critical heat flux for ignition was found to be 15 kW/m^2; and 14 kW/m^2 for sample C when tested in parallel to the grain. The temperature for ignition was calculated using equation (8). Total heat transfer coefficient was defined as 37.3 W/m^{2}K following the regression proposed by Hidalgo [34], which is based on a convective coefficient for horizontal hot plates and an emissivity of 0.8-1.0.

By plotting the inverse of the square root of the time to ignition against the external heat flux, the slope of the plot was obtained and, equation (6) was used to calculate the thermal inertia ($k\rho C_p$).. The results for the temperature of ignition T_{ig}, and thermal inertia can be seen in Table 3.

Table 3. Ignition parameters for laminated bamboo samples

Sample	q_{cr} [kW/m^2]	T_{ig} [°C]	$k\rho C_p$ [kW^{2}s/m^{4}K^2]
S.A_PP1	15	388	0.80
S.B_PP1	15	377	0.71
S.C_PP1	15	386	0.61
S.C_PP2	15	383	0.69
S.C_PLL	14	368	0.79

Limited information on the flammability parameters of laminated bamboo, can be found in literature, so Lateral Ignition Flame Spread (LIFT) apparatus was used by Mena *et al.* to test Guadua species in a vertical orientation [35]. Their data for the critical heat flux for ignition is in very good agreement with the results of the present study.

Table 4 shows values of timber as a benchmark to compare the properties of laminated bamboo.

Lateral Ignition Flame Spread (LIFT) apparatus was used by Mena *et al.* to test Guadua species in a vertical orientation [35]. Their data for the critical heat flux for ignition is in very good agreement with the results of the present study.

Table 4 Laminated bamboo in comparison with timber species from literature.

Sample	q_{cr} [kW/m^2]	T_{ig} [°C]	$k\rho C_p$ [kW^{2}s/m^{4}K^2]	Ref

Laminated Bamboo (Guadua)	14	-	-	[35]
Laminated Bamboo (Moso)	6	297	-	[36]
Laminated Bamboo (Moso)	14-15	450-485	0.32-0.37	[37, 38]
Macrocarpa	13	362	0.39	[39]
Beech	10.7	327	0.59	
Radiata Pine	8.1	281	0.81	
Rimu	7.8	275	1.29	
Mahogany	13.2	375	-	[40]
Douglas Fir [vertical Cone calorimeter]	13.2	350	0.159	[41]
Blackbutt [vertical Cone calorimeter]	10	300	0.394	[41]

Roberts [37] conducted his tests by means of the Cone Calorimeter and performed his data analysis in a similar fashion with the same values of critical heat flux results, but a temperature ignition almost 100 ºC higher. It is important to highlight that Roberts used a lower heat transfer coefficient, which could have contributed to obtaining a higher temperature for ignition and lower thermal inertia. Xu *et al.* [36] reported a critical heat flux of 6 kW/m^2, not in agreement with the data presented here or reported by Mena *et al.* and Roberts.

When compared to timber, laminated bamboo studied herein yielded higher values of the critical heat flux for ignition and temperature for ignition. Janssens measured the temperature for ignition through direct measurements, and his values are close to the results obtained through the model of ignition, as per equations (6) and (8). All other species exhibited less favourable parameters, indicating that more energy is required to ignite a sample of laminated bamboo, at higher temperatures, than the rest of the timber samples in this table. As for the thermal inertia, Lateral Ignition Flame Spread (LIFT) apparatus was used by Mena *et al.* to test Guadua species in a vertical orientation [35]. Their data for the critical heat flux for ignition is in very good agreement with the results of the present study.

Table 4 shows that Rimu and Moso reached virtually the same value thus present the highest resistance to temperature increase.

3.3.Burning rates

Figure 3 presents a plot of the critical mass loss rate versus external heat flux. Each point represents the average of two to three repeats at the same test condition. The values between the different samples range from 2 to 4.5g/m^2s. Sample B_PP1 in Figure 3 shows to have the lower values of critical mass loss rate for ignition, all tests yield values below 3.5 g/m^2s. Each point represents the average of two to three repeats at the same test condition. The values between the different samples range from 2 to 4.5g/m^2s. Sample B_PP1 in Figure 3 shows to have the lower values of critical mass loss rate for ignition, all tests yield values below 3.5 g/m^2s.

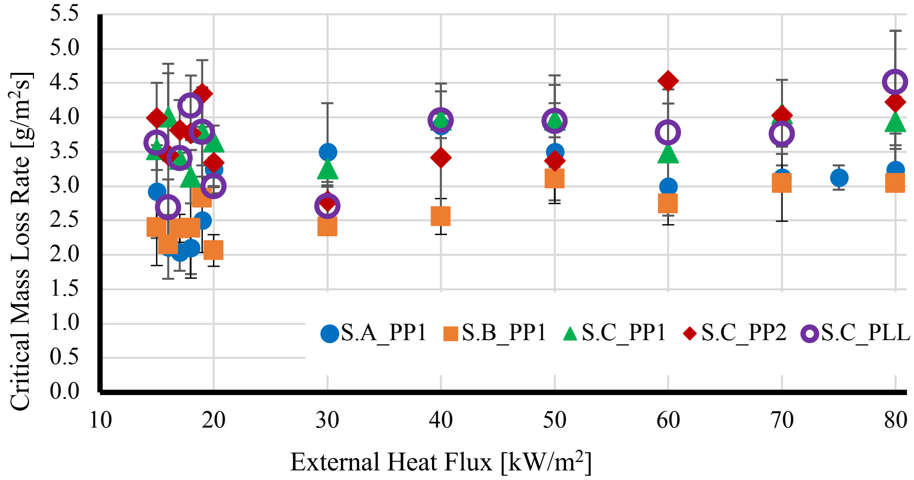

Figure 3 $\dot{m}''_{cr}$ (g/m^{2}s) vs $\dot{q}''_e$ kW/m^2 for sample A, B and C analysed for each method.

Sample C depicted higher values of critical mass loss rate than Sample A and B. For the side tested PP1 all data was above 3.0 g/m^{2}s. The lowest value of critical mass loss rate for ignition was found to be 3.1 g/m^{2}s tested at 18 kW/m^2. For side PP2 the minimum was 2.8 g/m^{2}s, tested at 30 kW/m^2, and 4.2 g/m^{2}s tested at 80kW/m^2. Side PLL has again higher values of critical mass loss rate, with the lowest value being 2.7 kW/m^2 tested at 16 kW/m^2 and the highest value of 4.5 g/m^{2}s tested at 80 kW/m^2. To the author's best knowledge, there is no data in regards to the critical mass loss rate of bamboo at the fire-point for reference. For comparison purposes, Table 5 summarises data obtained from other authors on timber products. The data presented for sample A, B and C is referenced to the highest value obtained and the heat flux at which they were tested.

Table 5 Comparison critical mass loss rate for ignition from literature.

Material	$\dot{m}''_{cr}$ [g/m2s]	Heat Flux/ Temperature	Ref
S.A_PP1	3.7	40 kW/m^2	-
S.B_PP1	3.1	50 kW/m^2	-
S.C_PP1	4.0	80 kW/m^2	-
S.C_PP2	4.0	80 kW/m^2	-
S.C_PLL	4.8	80 kW/m^2	-
Plywood	3.4	25-35 kW/m^2	[42]
Mahogany	1.8	18.8 kW/m^2	[43]
Oak, Pine, etc.	5.1	525 °C	[44]

Delichastsios [42] tested plywood to obtain the critical mass flux for ignition and its dependency on oxygen concentration variations. He obtained a mass loss rate of 3.4 g/m^{2}s for heat fluxes of

25 and 35 kW/m^2. When tested for 50 kW/m^2 he reported that the values ranged from 3.5 g/m^{2}s to more than 6 g/m^{2}s. Mass loss rate at the fire-point for White pine, Mahogany and deal panels was measured by Mazhar [45], Atreya et al. [43], and Bamford et al. [19], respectively. All these studies reported lower results than those presented herein. Koohyar et al. also tested a range of wood samples including Oak and Pine, although they report the critical mass loss for ignition in a range between 1-22 g/m^{2}s, with a mean value of 5.1 [21, 44]. According to Rasbash *et al.*, these previous works had no systematic experimental methods, and could have generated inconsistent results [24].

3.4.Heat Release Rates

This section presents the results of the peak value and the average values of the heat release rate per unit area over a period of one hour for sample B_PP1 and sample C for sides PP1, PP2 and PLL. The results of experiments tested at an external heat flux of 20, 40, 60 and 80 kW/m^2 are presented. Sample A is not reported in this sections because after 900 seconds the thermal wave had reached the back of the sample (Table 2), and simplifications detailed in section 2 were no longer be valid.

Good uniformity and repeatability can be observed from Figure 4 for the results of each test performed for sample B. When tested under an incident heat flux of 20 kW/m^2, tests lasted around thirty minutes. When tested at 80 kW/m^2, no flame out was observed and tests went on until burnout. The values for the heat flux 20, 40 and 60 kW/m^2 Figure 4 shows that at the end of the test, the Heat Release Rate drops to a value of zero. It is important to clarify that as explained in section 2.1, the samples were removed before the data collection finished, to be able to guarantee that the values of the oxygen concentration returned to the calibrated value, to guarantee reliable results. The oxygen concertation was also verified for the tests at 80 kW/m^2; however, the collection of data stopped tracking the Heat Release Rate before finishing the test.

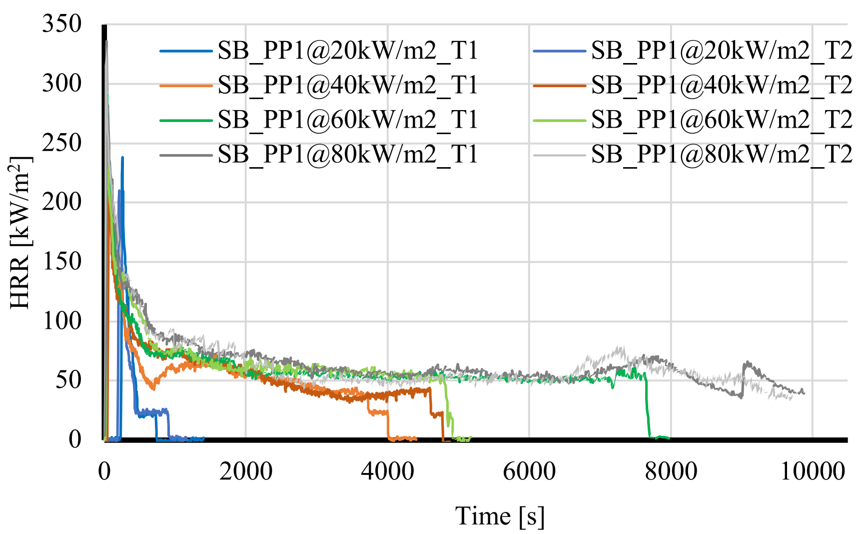

Figure 4 HRR Sample B for tests at 20, 40, 60, and 80 kW/m^2

To detail the behaviour of the heat release rate in bamboo, Figure 5 shows the results of two tests of Sample C performed on side PP1 at 40 kW/m^2. Both tests show very good repeatability. Ignition starts at early stages around 40-50 seconds. After ignition, the heat release rate increases steeply to a maximum value of 205 kW/m^2. After 160 seconds from the start of the test, it quickly drops down to a value of 100 kW/m^2. This sudden drop happens because a char layer starts to form on the surface of the specimen and acts as an insulation barrier protecting the virgin material and reducing the degradation rate. Once the char is formed, flames start to decrease until the sample reaches a quasi-steady burning.

From Figure 5, the quasi-steady state can be observed after the heat release rate per unit area reaches a value of 50 kW/m^2 at around 1,000 seconds. The heat release rate per unit area drops finally to a value of 40 kW/m^2 until the concentration of the volatiles start to reduce and the flame is extinguished at around 3,900 seconds. Once flameout has occurred smouldering combustions keeps generating a heat release rate per unit area of 25 kW/m^2 until the sample is removed from the combustion chambers, and the values drop to zero. As indicated above, this final step is to guarantee the correct readings for the baseline data.

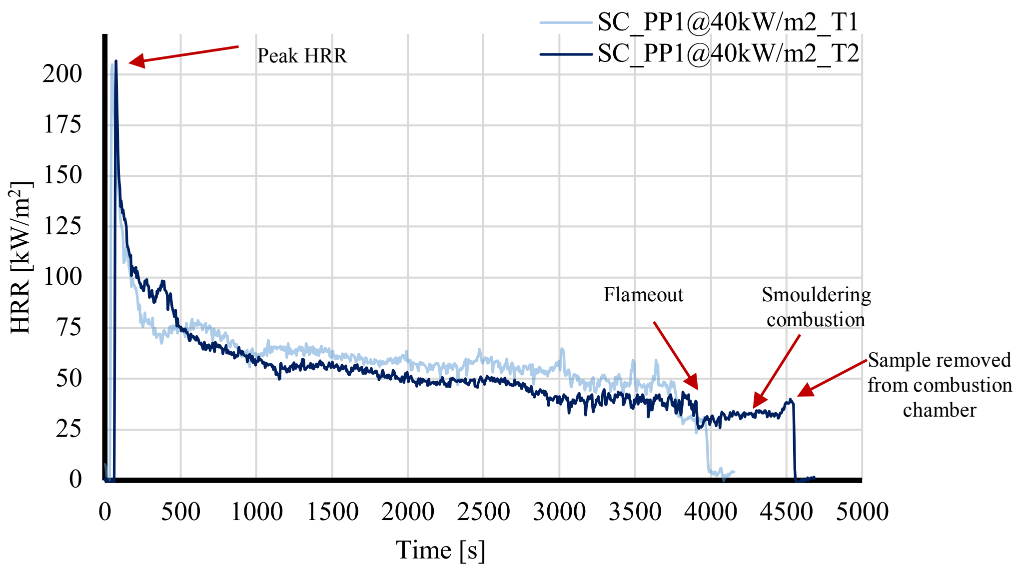

Figure 5 Heat Release Rate per Unit Area for sample SC_PP1 at 40 kW/m^2

Figure 6 shows representative values of the peak HRRPUA within the range of heat fluxes that can be expected in a real fire.

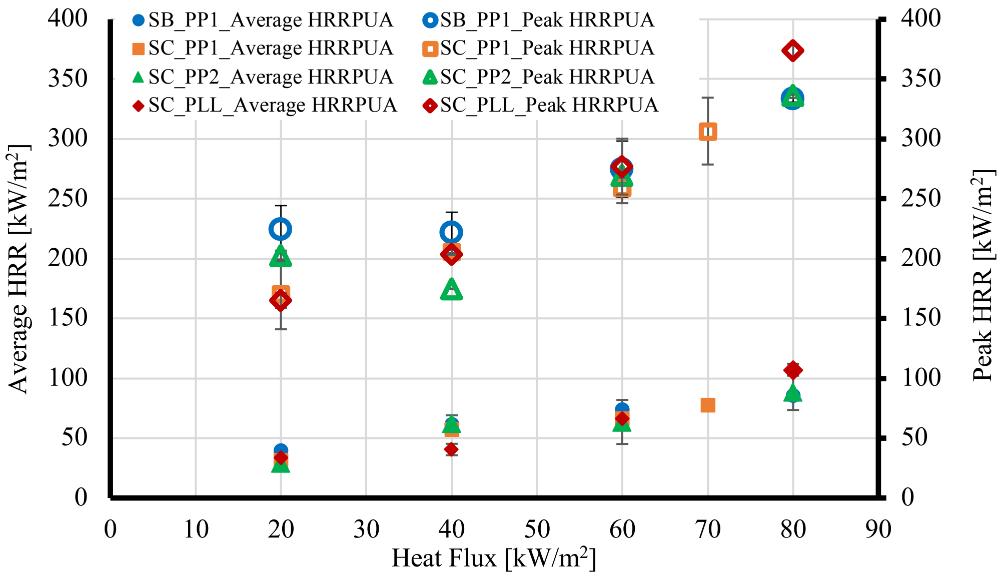

Figure 6 Average and Peak HRRPUA for Sample B and C at 20, 40, 60 and 80kW/m^2

4. Conclusions

This study has conducted a characterization of bamboo under conditions that are consistent with common approaches to flammability. All assumptions have been presented and results have been obtained to demonstrate the validity and limits of these assumptions. Ignition, critical mass flux for the fire point and HRRPUA have been fully quantified and compared with similar construction materials such as different species of wood.

Among the ignition parameters, effective thermal inertia results showed the highest variability. This is due to the high sensitivity of the methodology to small variations when calculating the slope of the time to ignition vs heat flux plots. In any case, mixed results are obtained when these parameters are compared to other bamboo sources. Overall, critical heat flux for ignition can be located at around 14 – 15 KW/m^2. Ignition temperature and effective thermal inertia shows higher variability nevertheless consistency is still found between different tests and other reported experimental results. The variability can be explained by the fact that slightly different testing methodologies were followed on each case.

Due to the uncertainties of determining the surface temperature during a test in an accurate way, the critical mass loss rate has been established as a reliable parameter to determine the onset of ignition. Good consistency between samples and good repeatability in each case allowed establishing the critical mass loss rate of laminated bamboo between 2 – 4.5 g/m^{2}s. In general terms, for all cases critical mass loss rate is lower for heat flux below 20 kW/m^2, and higher for higher heat fluxes. Comparison between different samples tested under the same orientation, allowed to conclude that Sample C tested parallel to the grain has the higher mass loss rate at ignition. There are no available references in literature regarding critical mass loss rates of bamboo.

Heat release rates per unit area were also very consistent between types of samples. In all cases, the peak value was reached early in the test and the measurements dropped very steeply soon after. This behaviour is attributed to the generation of a char layer at the surface that acts as an insulation layer, preventing temperature from building up in the virgin material. As expected, both average and peak heat release rates per unit area exhibited an upwards tendency for increasing values of incident heat flux. Sample C generates the largest absolute energy upon heating.

Laminated bamboo undergoes a long flaming stage followed by an even longer smouldering combustion process during which the heat release rate per unit are was sustained at 25 KW/m^2 in average. However, these results were affected by the frame holder. The flame holder needed to be placed on top of the sample to prevent the first lamella from getting closer to the heating cone. This effect caused by delamination must be taken into consideration in a real case scenario for design purposes.

Last, comparison of the results presented herein with timber materials must be done with caution, as bamboo is a completely different material. However, qualitative data suggests that laminated bamboo has better ignition properties, especially when observing that it presents higher critical heat flux and surface temperature for ignition than the references found in the literature review.

5. Acknowledgements

Non-financial support for this research was provided by several individuals and companies and we would like to highlight in particular Moso International BV and Yes Bamboo. The authors gratefully acknowledge The University of Queensland's Centre for Future Timber Structures for its support throughout this research; as well as Dr Andres Osorio, Jeronimo Carrascal, Dr Cristian Maluk, Mateo Gutierrez, Ian Pope, Tam Do, and the rest of the UQ Fire Research Team for their feedback and motivation.

6. References

1. Liu, X., et al., *Nomenclature for engineered bamboo.* BioResources, 2015. **11**(1): p. 1141-1161.
2. Van der Lugt, P. and J. Vogtländer, *The environmental impact of industrial bamboo products. Life cycle assessment and carbon sequestration.* Report Number: INBAR Technical Report, 2015. **35**.
3. BV, M.I. [cited 2019 1 August 2019]; Laminated bamboo Images]. Available from: https://www.moso.eu/en/products/beam-panel-veneer/solid-beam#
4. Jyoti Nath, A., G. Das, and A.K. Das, *Above ground standing biomass and carbon storage in village bamboos in North East India.* Biomass and Bioenergy, 2009. **33**(9): p. 1188-1196.
5. Van der Lugt, P., A.A.J.F. Van den Dobbelsteen, and J.J.A. Janssen, *An environmental, economic and practical assessment of bamboo as a building material for supporting structures.* Construction and Building Materials, 2006. **20**(9): p. 648-656.
6. Sharma, B., et al., *Mechanical characterisation of structural laminated bamboo.* Proceedings of the Institution of Civil Engineers-Structures and Buildings, 2016. **170**(4): p. 250-264.
7. Xiao, Y. and B. Sharma, *15-Engineered Bamboo. 2016*. Elsevier Ltd.
8. Li, X., *Physical, chemical, and mechanical properties of bamboo and its utilization potential for fiberboard manufacturing.* 2004.

9. Sharma, B., et al., *Engineered bamboo for structural applications.* Construction and Building Materials, 2015. **81**: p. 66-73.
10. Van der Lugt, P., *Design interventions for stimulating bamboo commercialization-Dutch Design meets bamboo as a replicable model.* 2008.
11. ISO-5660-1, *Reaction-to-fire tests. Heat release, smoke production and mass loss rate. Heat release rate (cone calorimeter method) and smoke production rate (dynamic measurement)*, in *BS ISO 5660-1:2015*. 2015, International Organization for Standardization: Geneva, Switzerland.
12. Lindholm, J., A. Brink, and M. Hupa, *Cone calorimeter—a tool for measuring heat release rate.* Åbo Akademi Process Chemistry Centre: Turku, Finland, 2009.
13. Torero, J., *Flaming ignition of solid fuels*. 2016.
14. Steinhaus, T., *Determination of intrinsic material flammability properties from material tests assisted by numerical modelling.* 2010.
15. Long, R., et al., *Scale and transport considerations on piloted ignition of PMMA.* Fire Safety Science, 2000. **6**: p. 567-578.
16. de Ris, J.L. and M.M. Khan, *A sample holder for determining material properties.* Fire and Materials, 2000. **24**(5): p. 219-226.
17. Drysdale, D., *An introduction to fire dynamics*. 2011: John Wiley & Sons.
18. Carslaw, H.S. and J.C. Jaeger, *Conduction of heat in solids.* Oxford: Clarendon Press, 1959, 2nd ed., 1959.
19. Bamford, C.H., J. Crank, and D.H. Malan, *The combustion of wood. Part I.* Mathematical Proceedings of the Cambridge Philosophical Society, 1946. **42**(2): p. 166-182.
20. Murty Kanury, A., *Ignition of Cellulosic Solids: Minimum Pyrolysate Mass Flux Criterion.* Combustion Science and Technology, 1977. **16**(1-2): p. 89-89.
21. Rasbash, D. *The relevance of firepoint theory to the evaluation of the fire properties of combustible materials*. in *Proc. Int. Symposium on the Fire Safety of Combustible Materials*. 1975. Edinburgh University.
22. Rasbash, D. *Theory in the evaluation of fire properties of combustible materials*. in *Proceedings of the Fifth International Fire Protection Seminar, Karlsruhe, Germany*. 1976.
23. Drysdale, D., *Ignition: the material, the source and subsequent fire growth*. 1983: Society of Fire Protection Engineers.
24. Rasbash, D., D. Drysdale, and D. Deepak, *Critical heat and mass transfer at pilot ignition and extinction of a material.* Fire Safety Journal, 1986. **10**(1): p. 1-10.
25. Tewarson, A., *Generation of heat and chemical compounds in fires.* SFPE handbook of fire protection engineering, 2002: p. 82-161.
26. Janssens, M.L., *Measuring rate of heat release by oxygen consumption.* Fire technology, 1991. **27**(3): p. 234-249.
27. Babrauskas, V. and R.D. Peacock, *Heat release rate: the single most important variable in fire hazard.* Fire safety journal, 1992. **18**(3): p. 255-272.
28. Thorton, R., *The relation of oxygen to the heat of combustion of organic compounds.* Philosophical Magazine Series, 1917. **33**: p. 196-203.
29. Parker, W.J., *Calculations of the heat release rate by oxygen consumption for various applications.* Journal of fire sciences, 1984. **2**(5): p. 380-395.
30. Huggett, C., *Estimation of rate of heat release by means of oxygen consumption measurements.* Fire and Materials, 1980. **4**(2): p. 61-65.

31. Babrauskas, V., *Development of the cone calorimeter—a bench-scale heat release rate apparatus based on oxygen consumption.* Fire and Materials, 1984. **8**(2): p. 81-95.
32. Babrauskas, V. and W.J. Parker, *Ignitability measurements with the cone calorimeter.* Fire and Materials, 1987. **11**(1): p. 31-43.
33. ASTM-E1354, *Standard test method for heat and visible smoke release rates for materials and products using an oxygen consumption calorimeter.* 2011.
34. Hidalgo-Medina, J.P., *Performance-based methodology for the fire safe design of insulation materials in energy efficient buildings.* 2015.
35. Mena, J., et al., *Assessment of fire reaction and fire resistance of Guadua angustifolia kunth bamboo.* Construction and Building Materials, 2012. **27**(1): p. 60-65.
36. Xu, Q., et al., *Combustion performance of engineered bamboo from cone calorimeter tests.* European Journal of Wood and Wood Products, 2017. **75**(2): p. 161-173.
37. Roberts, C., *The Thermomechanical Response of Laminated Bamboo to Constant Heat Fluxes* 2016, The University of Edinburgh.
38. Bartlett, A.I., et al. *Thermal and flexural behaviour of laminated bamboo exposed to severe radiant heating*. in *2018 World Conference on Timber Engineering*. 2018.
39. Ngu, C.K., *Ignition Properties of New Zealand Timber*, in *School of Engineering*. 2001, University of Canterbury p. 131.
40. Atreya, A., C. Carpentier, and M. Harkleroad, *Effect of sample orientation on piloted ignition and flame spread.* Fire Safety Science, 1986. **1**: p. 97-109.
41. Janssens, M., *Fundamental thermophysical characteristics of wood and their role in enclosure fire growth*. 1991, Ghent University.
42. Delichatsios, M.A., *Piloted ignition times, critical heat fluxes and mass loss rates at reduced oxygen atmospheres.* Fire Safety Journal, 2005. **40**(3): p. 197-212.
43. Atreya, A. and I. Wichman, *Heat and mass transfer during piloted ignition of cellulosic solids.* Journal of Heat Transfer, 1989. **111**(3): p. 719-725.
44. Koohyar, A., J. Welker, and C. Sliepcevich, *The irradiation and ignition of wood by flame.* Fire Technology, 1968. **4**(4): p. 284-291.
45. Thomson, H. and D. Drysdale, *Critical mass flowrate at the firepoint of plastics.* Fire Safety Science, 1989. **2**: p. 67-76.